Supporting Information

Gillet et al. 10.1073/pnas.1111840108

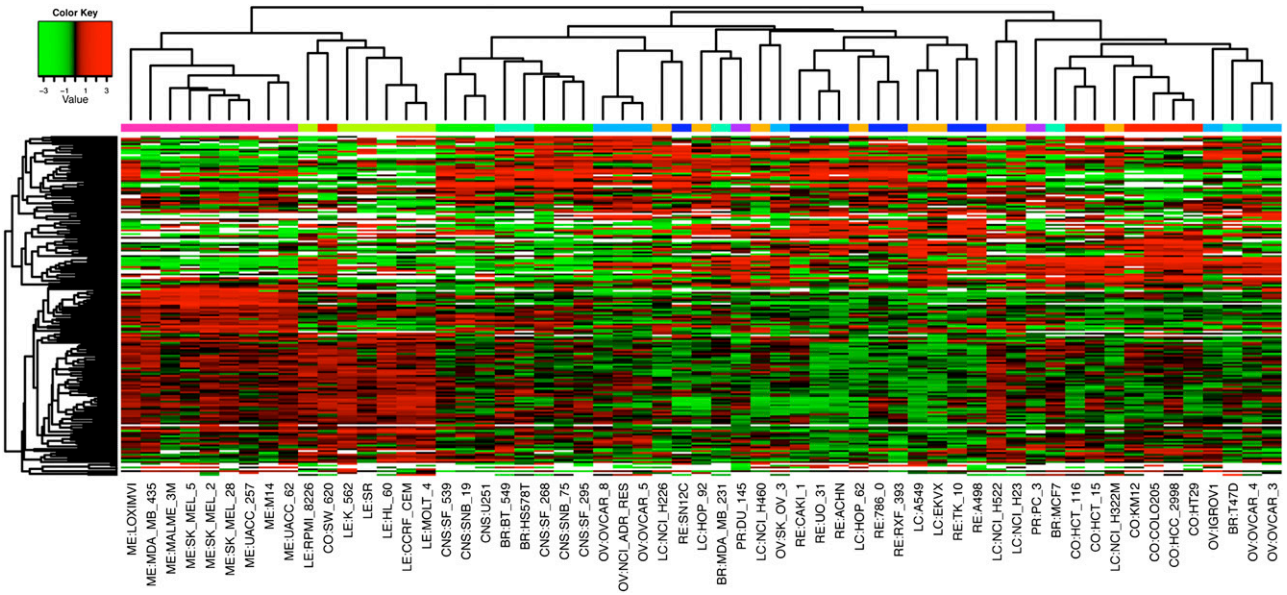

Fig. S1. Heterogeneity among the cell lines within a tumor type of the NCI-60 panel. Hierarchical clustering performed using 185 genes that are found differentially within the nine cancer types representing the NCI-60 panel. *x* axis: magenta, melanoma; light green, leukemia; dark green, CNS; turquoise, breast cancer; blue, ovarian cancer; orange, non-small cell lung cancer; dark blue, renal cancer; purple, prostate cancer; red, colon cancer. The *y* axis shows gene clustering.

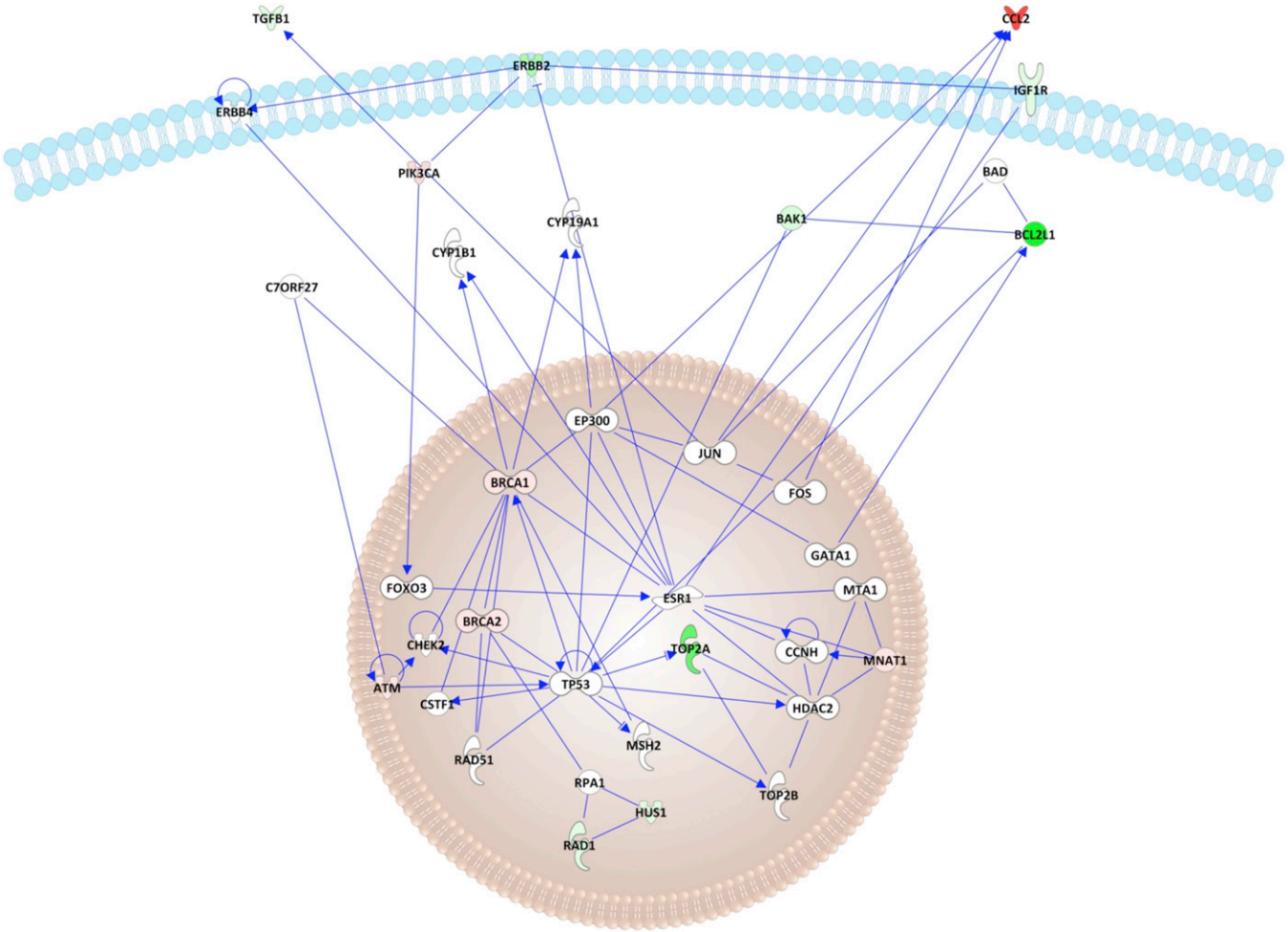

Fig. S2. Pathway analysis of the gene signature found in the ovarian cancer cell lines of the NCI-60 panel. The highest-ranked pathway derived from the IPA software indicated the activation of the p53 pathway.

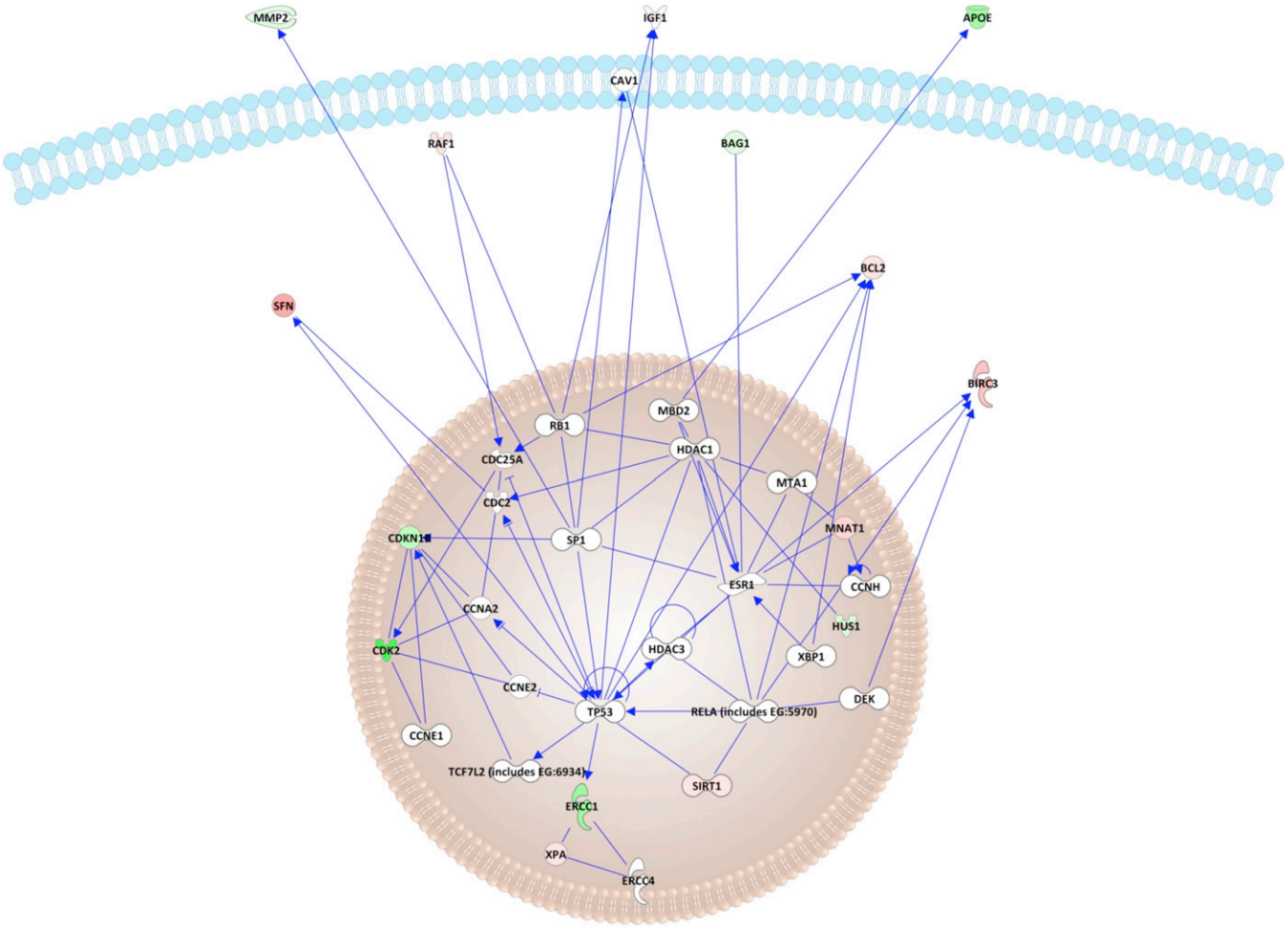

Fig. S3. Pathway analysis of the gene signature found in the melanoma cell lines of the NCI-60 panel. This was the second highest ranking network derived from the IPA software analysis.

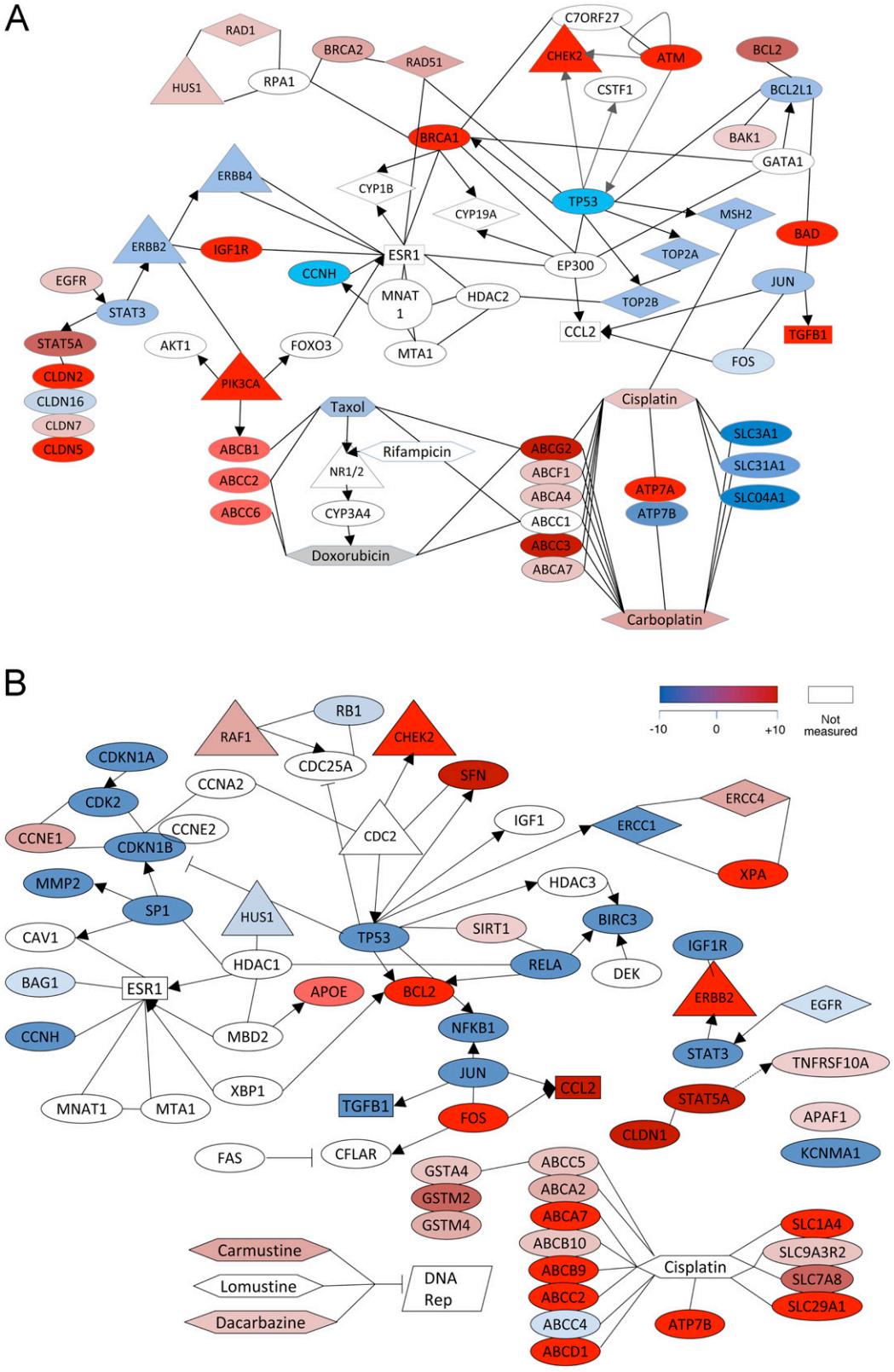

Fig. S4. Pathway analysis of the gene signature found in the ovarian and melanoma cell lines of the NCI-60 panel. Pathways enhanced using SIMUSITE (BioPhase Systems) (*A*) Pathway of the ovarian cancer cell line, IGROV-1 as a model. (*B*) Pathway of the melanoma cell line, Lox-IMV1.

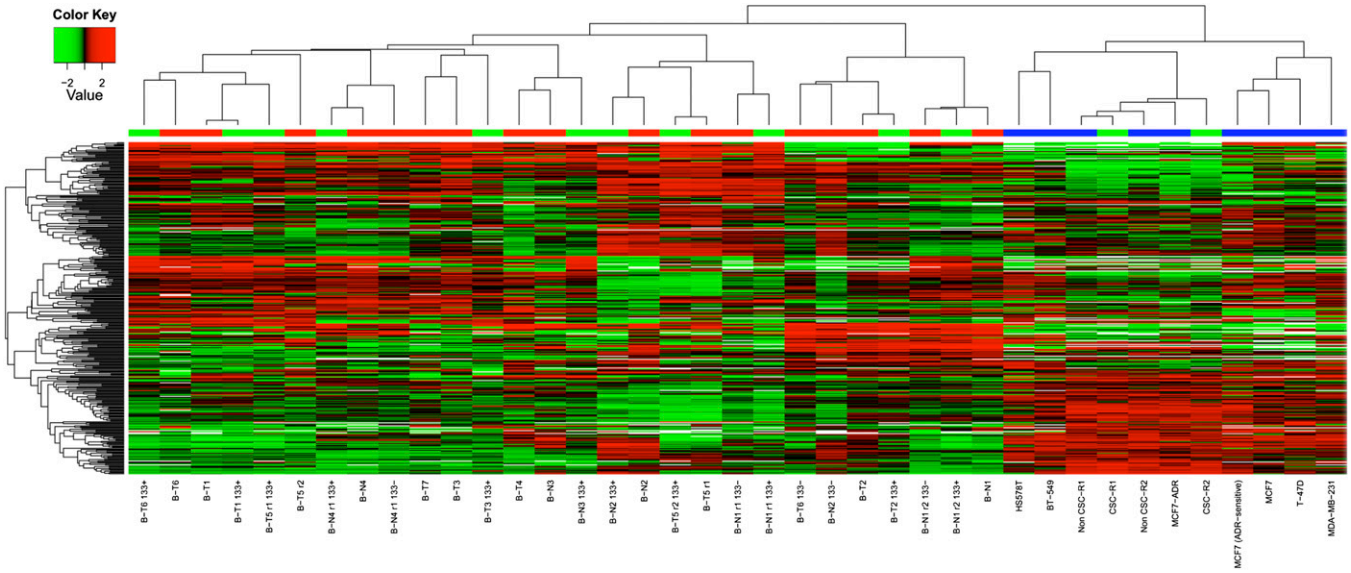

Fig. S5. Hierarchical clustering (using the average linkage algorithm and 1-Pearson correlation as the distance measure) reveals two distinct clusters that discriminate between the in vitro models (cancer cell lines of the NCI-60 panel) and the clinical samples. Gene expression profiles of $CD133^+$ cancer-stem-like cells (green bars) isolated directly from surgical samples were not distinguishable from those of the breast cancer as a whole, and were different from those of either stem-cell–like populations found among MCF-7 drug-resistant cells, the entire population of MCF-7 cells, and other cultured breast cancer cells. Heatmap of seven clinical samples of breast cancer, four samples of normal breast tissue (red bars), and seven breast cancer cell lines (blue bars), including two replicates of isolated cancer stem-like cells (green bars) from MCF7-ADR–resistant cancer cells. Replicates were also performed for clinical samples and are labeled "r". Cancer stem-like cells were isolated from clinical samples by using the following method: Tumors and normal tissues obtained from the Cooperative Human Tissue Network were weighed and washed in ice-cold RPMI containing antibiotic and antimycin medium. The tissues were minced and incubated in a medium containing collagenase IV (2 mg/mL and digested for 4–6 h at 37 °C in a water bath. The digestion was carried out for 2 h in a 50-mL tube, and the volume varied between 5 and 25 mL, depending on the size of the sample. The suspension was filtered with a 100-μm filter to remove cell debris. The suspension was kept at 5 °C to remove the fat material forming a ring at the top and incubated for 20 min at 37 °C in solution containing Accutase (1 mg/mL), then filtered with a 40-μm filter and centrifuged at 100 × *g* for 10 min. The pellet was washed and resuspended in HBSS/BSA. The resuspended cells were incubated with CD133-conjugated beads without azide (50 μL of beads per 10^7 cells) at 0 °C for 30 min. The $CD133^+$ cells were finally isolated by using MACS separation columns as per the manufacturer's instructions (Miltenyi Biotec). Unattached cells that passed through the column were labeled $CD133^-$.

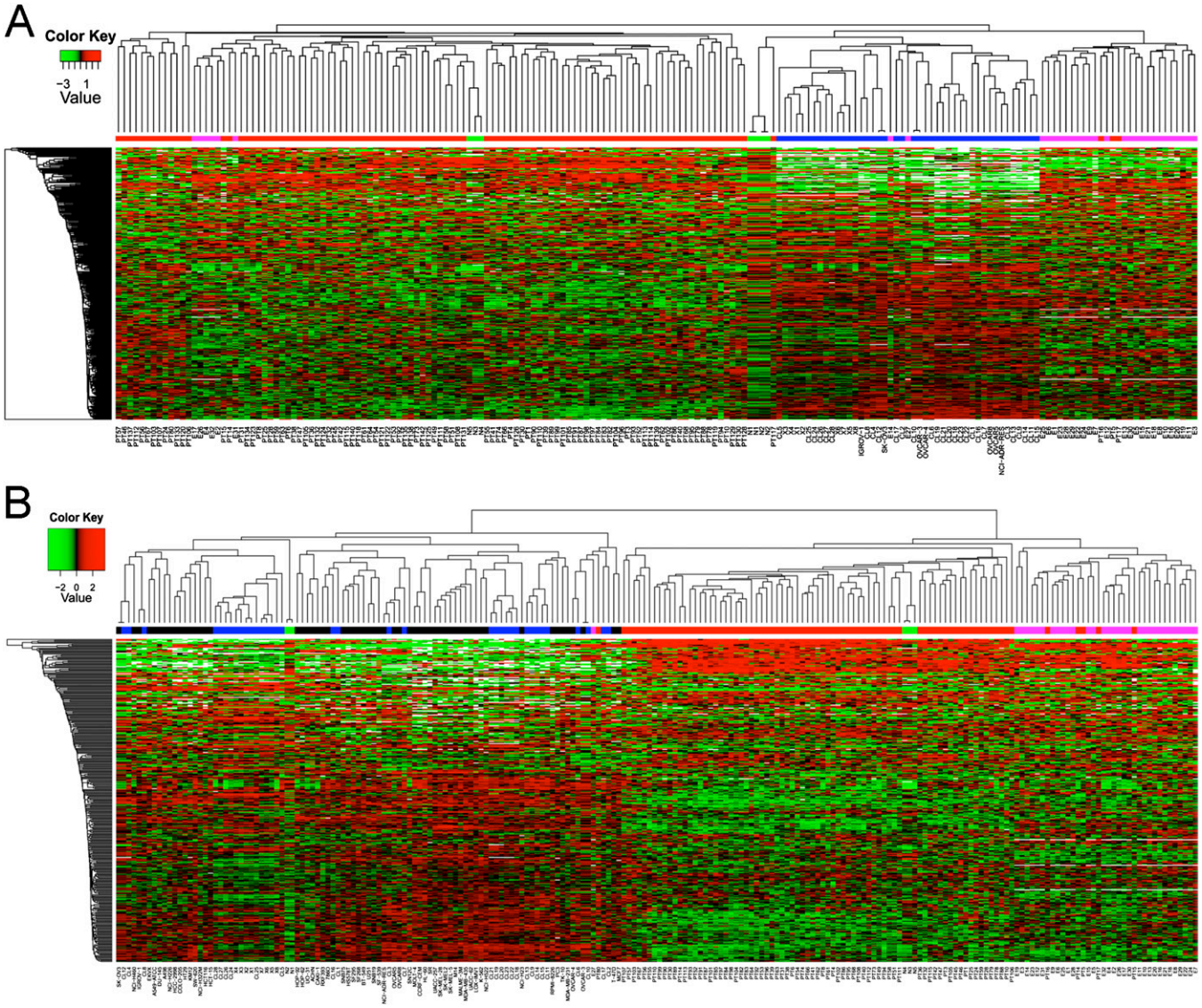

Fig. S6. Hierarchical clustering using Euclidean distance of the ovarian cancer samples analyzed. (*A*) The 380 MDR-linked gene expression profile (measured by using Taqman low density array) of ovarian cancer models (in vitro and in vivo) is strikingly different from that of specimens of untreated ovarian primary serous carcinoma taken from 80 patients and 32 effusion samples originating from primary ovarian serous carcinoma. The *x* axis shows clusters of samples. Red, primary ovarian serous carcinoma; magenta, effusion samples originating from primary ovarian serous carcinoma; green, normal ovarian tissue; blue, in vitro models of ovarian cancer, including xenograft models of ovarian cancer (X), ovarian cancer cell lines of the NCI-60 panel, and cisplatin-resistant cell lines. The *y* axis shows gene clustering. (*B*) When adding the eight additional cancer types of the NCI-60 panel to the heatmap presented in *A*, the striking observation is made that all of the cell lines either grown in vitro or in vivo bear more resemblance to each other, regardless of the tissue of origin, than to the clinical samples that they are supposed to model. Along the *x* axis: red, primary ovarian serous carcinoma; magenta, effusion samples originating from primary ovarian serous carcinoma; green, normal ovarian tissue; blue, in vitro models of ovarian cancer; black, cancer cell lines of the eight additional cancer types of the NCI-60 panel. The *y* axis shows gene clustering.

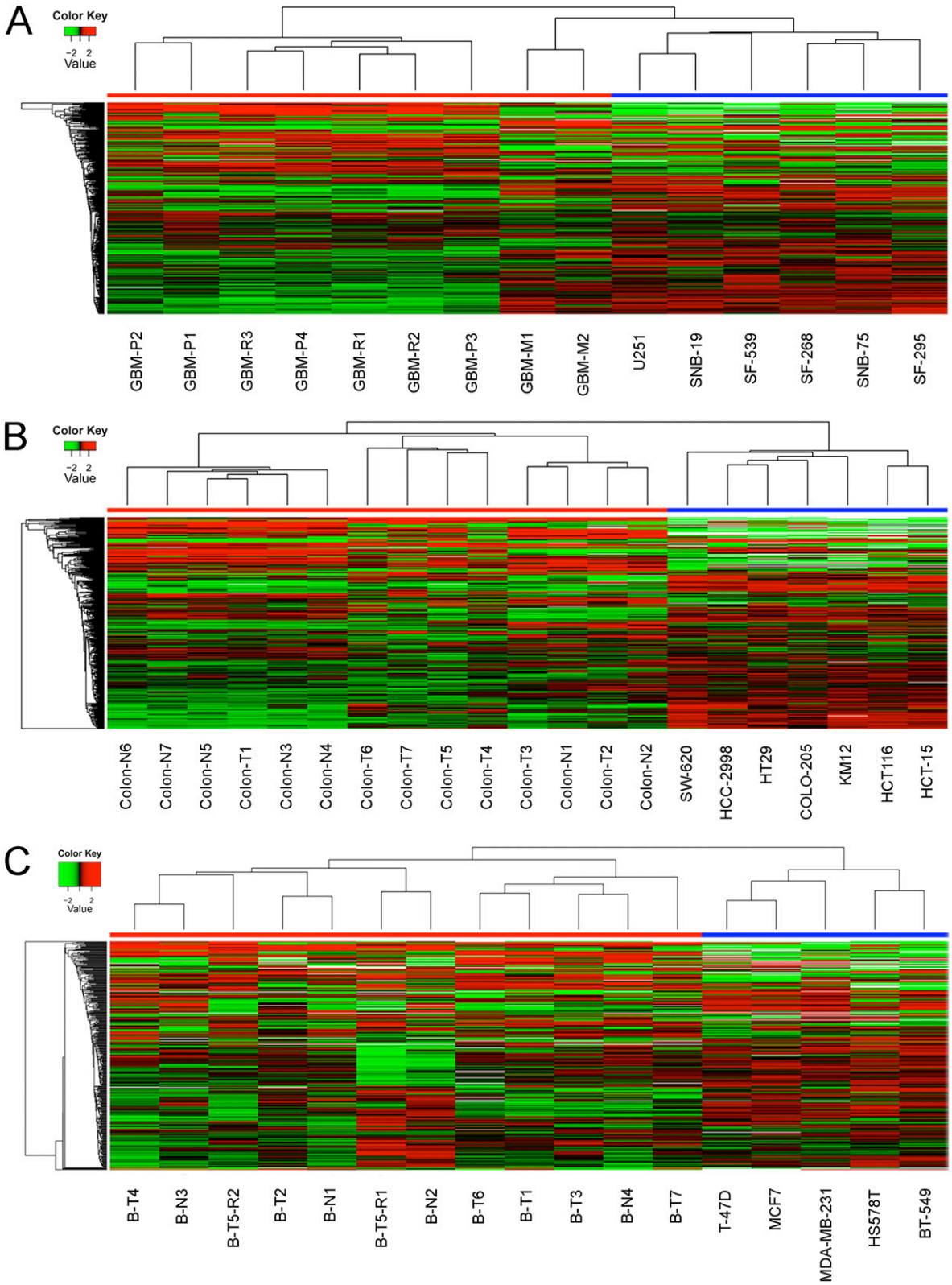

Fig. S7. (Continued)

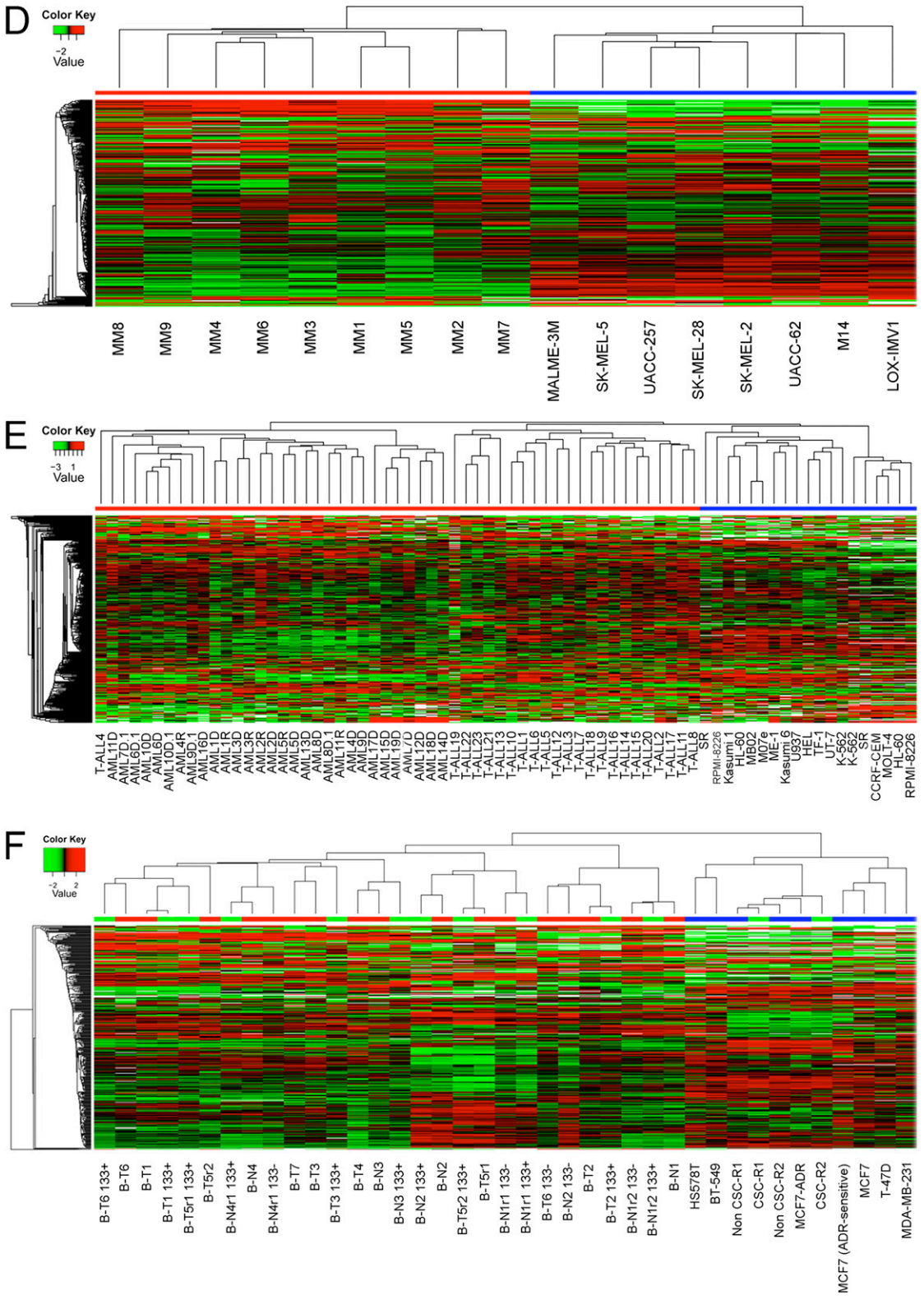

Fig. S7. Hierarchical clustering (using Euclidean distance) reveals two distinct clusters that discriminate between the in vitro models (cancer cell lines of the NCI-60 panel) and the clinical samples. (*A*) Heatmap of nine clinical samples of glioblastoma cancer, including four primary tumors, three recurrent tumors, and two metastases. (*B*) Heatmap of seven colon cancer samples paired with normal colon tissue taken during tumor resection. (*C*) Heatmap of 11 clinical samples of breast tissue, including four normal breast tissues and seven breast tumors. (*D*) Heatmap of nine metastic melanoma samples. (*E*) Heatmap generated from 23 T-acute lymphoblastic leukemia (12 were untreated, whereas 11 received conventional chemotherapy) and 11 paired samples of acute myeloid leukemia taken at diagnosis and after relapse. x axis: blue, cell lines; red, tumors. The y axis shows gene clustering. (*F*) Heatmap of seven clinical samples of breast cancer, four samples of normal breast tissue, and seven breast cancer cell lines, including two replicates of isolated cancer stem-like cells from MCF7-ADR-resistant cancer cells.

Other Supporting Information Files

Table S1 (DOC)
Table S2 (DOC)
Table S3 (DOC)
Table S4 (DOC)